Impurity-induced staggered polarization and antiferromagnetic order in spin-$\frac{1}{2}$ Heisenberg two-leg ladder compound $SrCu_2O_3$: Extensive Cu NMR and NQR studies

S. Ohsugi, Y. Tokunaga, K. Ishida, and Y. Kitaoka
Department of Physical Science, Graduate School of Engineering Science, Osaka University, Toyonaka, Osaka 560-8531, Japan

M. Azuma, Y. Fujishiro, and M. Takano
Institute for Chemical Research, Kyoto University, Uji, Kyoto-fu 611, Japan

(Received 13 October 1998; revised manuscript received 8 February 1999)

We report characteristics of impurity-induced staggered polarization (IISP) and antiferromagnetic long-range order (AF-LRO) in the gapped spin-1/2 Heisenberg two-leg ladder compound $SrCu_2O_3$ (Sr123). We have carried out comprehensive NMR and NQR investigations on three impurity-doped systems, $Sr(Cu_{1-x}M_x)_2O_3$ ($M=$Zn, Ni) with $x\leqslant 0.02$ and $Sr_{1-x}La_xCu_2O_3$ with $x\leqslant 0.03$. Either the Zn or Ni impurity that is nonmagnetic depletes a single spin on the ladders, whereas the La impurity is believed to dope electrons onto the ladders. The width of the Lorentzian Cu NMR spectrum increases with the increase in impurity content x and follows the Curie-like temperature (T) dependence as W/T. The W's for the Zn- and Ni-doped samples (M doping) are larger than for the La-doped one (La doping). The NMR spectra were fit by assuming that unpaired spin $S_0=1/2$ induced next to impurity on the rung for the Zn and Ni doping ($S_0=1/4$ for the La doping) creates the staggered spin polarization along the leg, which decreases exponentially from S_0. In Sr123, an instantaneous spin-correlation length ξ_0 was theoretically predicted as $\xi_0/a\sim 3-8$, where a is the lattice spacing between the Cu sites along the leg. However, a correlation length ξ_s/a estimated from the IISP along the leg was found to be much longer than ξ_0/a in $x=0.001$ and 0.005. The notable result is that ξ_s/a that was found to be T independent is scaled to mean distances $D_{AV}=1/(2x)$ between the Zn and Ni impurities and $D_{AV}=1/x$ between the La impurities. When $D_{AV}=500$ for $x=0.001$ (Zn doping), $\xi_s/a\sim 50$ is estimated. The significantly broadened NQR spectrum has provided unambiguous evidence for the AF-LRO in the Zn and Ni doping (x=0.01 and 0.02). Rather uniform AF moments at the middle Cu sites between the impurities are estimated to be about $0.04\mu_B$ at 1.4 K along the a axis. By assuming that exponential decay constants of AF moments are equivalent to ξ_s/a's for the IISP, the size of an AF moment next to the impurity is deduced as $S_{AF}\sim 1/4$. We propose that these exponential distributions of IISP and AF moments along the two-leg suggest that an interladder interaction is in a weakly coupled quasi-one-dimensional (WC-Q1D) regime. The formula of $T_N=J_0\exp(-D_{AV}/(\xi_s/a))$ based on the WC-Q1D model explains T_N(exp)=3 K ($x=0.01$) and 5.8 K ($x=0.02$) quantitatively and predicts to be as small as $T_N=0.09$ K for $x=0.001$ using $J_0=2000$ K. On the other hand, there is no evidence of AF-LRO for the La doping ($x=0.02$ and 0.03) down to 1.4 K, nevertheless their ξ_s/a's are almost equivalent to those in the Zn and Ni doping ($x=0.01$ and 0.02). We remark that the Q1D-IISP is dramatically enhanced by the interladder interaction even though so weak, once the impurity breaks up the quantum coherence in the short-range resonating valence bond (RVB) state with the gap. On the one hand, we propose that T_N is determined by a strength of the interladder interaction and a size of S_0. [S0163-1829(99)00530-5]

I. INTRODUCTION

Theoretical[1,2] and experimental[3–6] works unraveled the fact that $SrCu_2O_3$ (Sr123) is a typical gapped spin-1/2 quasi-one-dimensional (Q1D) Heisenberg two-leg ladder compound. In Sr123, the ladders, consisting of antiferromagnetic (AF) Cu-O-Cu linear bonds, are spatially connected with each other so that they form $2D-Cu_2O_3$ sheets.[3] Each ladder is magnetically decoupled because of the interladder 90° Cu-O-Cu bond causing the frustration in magnetic interaction at the interface. Even-leg spin-ladder systems have been established to be in a short-range resonating valence bond (RVB) ground state[1,2,7,8] with an instantaneous magnetic correlation length ξ_0 of only a few lattice spacings.[1,2] Measurements of the magnetic susceptibility χ,[4] the Cu nuclear spin-lattice relaxation rate T_1^{-1},[5] and the inelastic neutron scattering,[6] evidenced a large spin gap $E_g\sim 400$ K. Motivated by the theoretical conjecture that the singlet superconductivity should occur by lightly doping into the even-leg ladder system,[1,7,8] extensive experimental efforts have been devoted to discover the superconductivity in hole-doped two-leg spin-ladder systems. Meanwhile, Uehara *et al.* have discovered the superconductivity with $T_c=12$ K under a pressure of 3 GPa in $Sr_{0.4}Ca_{13.6}Cu_{24}O_{41.84}$.[9] In Sr123, however, neither hole nor electron doping has been successfully made yet. Although the La substitution for the Sr sites is believed to dope electrons onto the ladders, carriers are reported to be localized.[10]

Nonmagnetic impurity-induced antiferromagnetic long-range order (AF-LRO) in low dimensional quantum spin systems was first reported in the gapped spin-1/2 1D-Heisenberg AF magnet $CuGeO_3$[11,12] which exhibits the spin-Peierls (SP) transition.[11] Of particular interest is the coexistence of AF-LRO and lattice dimerization,[13,14] which has been theoretically interpreted in terms of the phase Hamiltonian by Fukuyama *et al.*[15]

Subsequently, Azuma *et al.*[16] and Nohara *et al.*[17] reported a surprising result through the measurements of $\chi(T)$ and specific heat $C(T)$ in Sr123. Only 1%-Zn substitution (denoted as Zn doping) for the Cu sites breaks up the singlet spin-liquid state and leads to an AF-LRO. Fukuyama *et al.* remarked that a nonmagnetic impurity replacing a spin in gapped two-leg spin-ladder systems induces a staggered spin modulation and leads to the AF-LRO in Sr123.[18] The collective spin-singlet ground state with the gap is stabilized due to the quantum coherence. It was therefore proposed to be due to this quantum coherence effect to be very susceptible to the randomness which results in the appearance of staggered magnetic modulation.[19]

In the Zn doping, the Néel temperature T_N undertakes a broad maximum at $T_N^{Max}\sim 8$ K around $x=0.04$.[16] Above T_N, a Curie behavior $\chi(T)=C/T$ and a T-linear specific heat $C_s=\gamma T$ have been observed.[17] A finite value of $\gamma \sim 3.5$ mJ/K^2 for $x=0.02$ and 0.04 suggested a gapless spin excitation. Inelastic neutron-scattering measurement revealed, on the other hand, that a singlet-triplet excitation gap $E_g\sim 400$ K (33 meV) is independent of x, although its integrated intensity decreases monotonically with increasing x.[6] This intimate variation of magnetic spectral weight (SPW) as the function of x was first noted for disordered spin-Peierls systems whose typical example is $CuGeO_3$ with a small amount of Zn replacing Cu or Si replacing Ge.[19,20] The SPW in the clean system has a well-defined gapped mode around the AF wave vector **Q**. As a small amount of disorder increases, however, the gapped mode undergoes an appreciable broadening and concomitantly a new SPW is introduced at low energies, $\omega\sim 0$ at **Q**. This disorder-induced low-energy SPW grows up with increasing x to become a well-defined Gold-stone mode of AF spin wave below T_N. At T_N or some critical x_c, even though AF-LRO disappears, its SPW still remains at $\omega\sim 0$. This interprets the presence of a finite γ value and of a seeming gapped mode.[14,21]

For the Zn doping, a magnitude of local moment estimated from $\chi(T)=C/T$ is about $0.75\mu_B$/Zn.[16] Nonmagnetic Zn^{2+} ion depletes a single spin on the rung. Therefore unpaired spin $S_0\sim 1/2$ was expected to be induced on the Cu site next to Zn on the same rung. Extensive theoretical studies have indicated that a nonmagnetic impurity induces the formation of a spin-1/2 local moment and the substantial enhancement of staggered spin correlation around the impurity.[18,22–25] Iino and Imada reported that the quantum Monte Carlo (QMC) results on ladders reproduces a Curie law, $\chi(T)=C/T$ and $C_s=\gamma T$, consistent with the experiments when x_c exceeding ~ 0.04. They did not, however, succeed to explain a finite value of γ and a persistence of AF-LRO down to a low doping level of Zn ($x=0.01$).[23] This is because a weak effective exchange coupling between unpaired spins decreases exponentially along the leg as $\exp(-r/\xi_0)$ where r is the distance from S_0 and $\xi_0/a\sim 3$. As a consequence, a 3D interladder coupling has been proposed to play an important role for the occurrence of AF-LRO.[26] They have put forth the scaling theory together with the QMC calculations. The scaling properties are characterized by the 3D strong interladder coupling, which is relevant for understanding the experimental results in the low doping level.[26]

Recently, Fujiwara *et al.* reported that the Cu NMR spectral width for the Zn doping ($x=0.0025$ and 0.005) increases with increasing x and varies as W/T with decreasing T. The NMR spectra in $T=30$–40 K were, however, not fit by assuming an impurity-induced staggered polarization (IISP) with a form of $S_i^z=(-1)^i S_0 \exp(-r_i/\xi_s)$ at a distance r_i from the impurity. In particular, the NMR spectral shape was never simulated with a larger ξ_s/a and $S_0\sim 1/2$, although it was noted that a possible correlation length ξ_s/a might be much longer than $\xi_0/a\sim 3$–8.[27]

Appearance of AF correlation enlarged by introducing a spin vacancy in 1D gapped spin-1/2 systems has been challenging to interpret. On the base of the computational techniques, Laukamp *et al.*[28] have studied the effect of spin vacancy, for example, a nonmagnetic Zn depleting a single spin on the ladders. It was shown that a staggered spin-spin correlation are markedly enhanced near these spin vacancies. Their results show that for $J_\perp/J_0=0.5$ and $x=0.014$, all the spins of ladder cluster with a (2×50) finite size have nonvanishing AF susceptibility. Here $J_\perp$ (J_0) is the exchange constant along the rung (leg).

In order to clarify these experimental and theoretical puzzling features on the IISP and the AF-LRO in the impurity-doped Sr123, we have carried out comprehensive Cu NMR and NQR studies on the Zn- and Ni-doped Sr123 (denoted as Zn and Ni doping) with $x\leqslant 0.02$ and the La-doped Sr123, $Sr_{1-x}La_xCu_2O_3$ (La doping) with $x\leqslant 0.03$. The La doping is believed to dope electrons onto the ladders. We have found that the impurity induces a staggered polarization along the leg. A striking result is that its correlation length ξ_s/a for a very small x is extended over a distance much longer than $\xi_0/a\sim 3$–8. At low temperature and zero field, the Cu NQR measurements have evidenced an AF-LRO for the Zn and Ni doping ($x=0.01$ and 0.02), but not for the La doping. We propose that T_N is determined by a strength of interladder interaction and a size of S_0.

II. EXPERIMENTAL PROCEDURES

Preparation techniques of samples were already described elsewhere.[16] The samples characterized by the powder x-ray diffraction were confirmed to keep their good quality. We used the c-axis oriented powder samples. The Cu NMR spectrum was obtained in $T=4.2$–286 K at 125.1 MHz by a sweeping magnetic field H with the use of a phase-coherent pulsed-NMR spectrometer and a superconducting magnet (12 T at 4.2 K). The Cu NQR spectrum at 1.4 K and $H=0$ was obtained by plotting a spin-echo intensity as a function of frequency ν point by point. The spin-echo intensity at each ν was corrected by the Boltzmann factor and the receiver sensitivity which was ν independent in $\nu=8-14$ MHz. Since the interval between 90° and 180° pulses τ in the spectrum measurements was so short with $\tau=13$ μsec, the corresponding correction upon ν was not made.

III. NMR RESULTS AND DISCUSSIONS

A. Cu NMR spectrum

The Cu NMR spectra at 150 K for $H\|c$ axis are indicated in Fig. 1 regarding the oriented powders of undoped Sr123

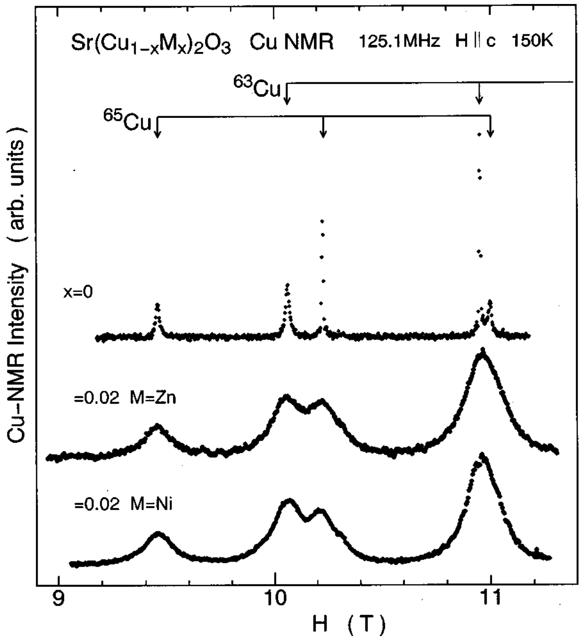

FIG. 1. The Cu NMR spectra for the *c*-axis oriented powders $Sr(Cu_{1-x}M_x)_2O_3$ ($M=$Zn, Ni) (M doping) with $x=0$ and 0.02 at 150 K for $H\|c$ axis. Arrows point to the peak positions of the spectra split by the first-order eqQ interaction for two isotopes ^{63}Cu and ^{65}Cu ($I=3/2$).

and the Zn and Ni doping ($x=0.02$). The spectra compose of several peaks due to the first-order effect of the nuclear electric quadrupole (eqQ) interaction for two isotopes ^{63}Cu and ^{65}Cu ($I=3/2$) as marked by arrows. The spectral width is fairly larger for the Zn and Ni doping than for Sr123. Figure 2 indicates $^{65}\Delta H/2$ vs T^{-1} plots. Here $^{65}\Delta H/2$ is defined as

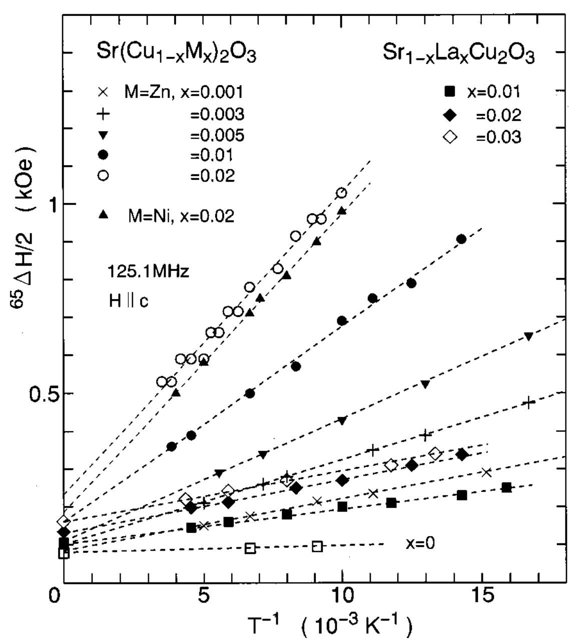

FIG. 2. $1/T$ dependence of $^{65}\Delta H/2$, a half width at the low-field side at the half intensity of peak arising from the ($3/2\leftrightarrow 1/2$) transition in the ^{65}Cu spectrum. Presented are those for the Zn ($x=0.001$–0.02) and Ni doping ($x=0.02$) and the La doping ($x=0.01$, 0.02, and 0.03) in $Sr_{1-x}La_xCu_2O_3$.

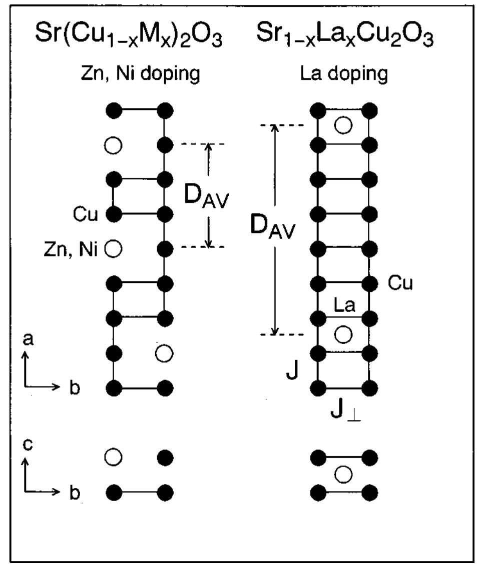

FIG. 3. Schematic coordination of impurities on the ladder for the Zn and Ni doping (left panel) and on the Sr layer for the La doping (right panel). Mean distance $D_{AV}=1/(2x)$ for the Zn and Ni doping and $1/x$ for the La doping.

the lower-field half width at the half intensity of peak in the ^{65}Cu NMR spectrum arising from the ($3/2\leftrightarrow 1/2$) transition. This peak does not overlap with the ^{63}Cu NMR spectrum whose width increases upon cooling and/or with some extrinsic signal arising from unaligned grains. Therefore a precise measurement is guaranteed. Apparently, the $^{65}\Delta H/2$ in Sr123 is almost T independent. By contrast, those for all samples follow the T dependence of

$$^{65}\Delta H=\frac{W}{T}+{}^{65}\Delta H_c. \qquad (1)$$

An extrapolated value to $T\rightarrow\infty$, $^{65}\Delta H_c$ is ascribed to some distribution of the *c*-axis component of quadrupole frequency $^{65}\Delta\nu_c$. This distribution originates from some inhomogeneous electric-field gradient (EFG) caused by doping impurities. In fact, $^{65}\Delta H_c$'s are in good agreement with those estimated from the Cu NQR spectrum as presented in the next section. W increases with increasing x as seen in Fig. 2. Note that the W at $x=0.02$ are almost the same for the Zn and Ni doping, but that for the La doping is smaller. The $^{65}\Delta\nu_c$'s for the Ni and La doping are smaller than that for the Zn doping.

Figure 3 illustrates a schematic configuration of the Zn and Ni (La) impurities on the ladder (Sr layer). Extensive theoretical works have reported that unpaired spin $S_0\sim 1/2$ is induced at the Cu site next to Zn or Ni on the same rung.[18,22–25] The $^{65}\Delta H/2$ varying as W/T suggests that S_0 polarized by H produces the IISP along the leg due to a large exchange interaction $J_0\sim 2000$ K.[29] The IISP develops as a staggered spin susceptibility $\chi'(\mathbf{q}=\mathbf{Q},\ \omega=0)$ increases upon cooling. Although the La doping does not deplete a spin on the ladders, doped electrons tend to localize on the ladders as suggested from the previous NMR study[5] and the resistivity measurement.[10] As a result that the spins of doped localized electrons couple with some Cu spins on the ladders, the spin degree of freedom is anticipated to emerge in the vicinity of the La impurity. W per impurity that is proportional to S_0 is very smaller for the La doping than for the Zn and Ni doping. We remark that doped electrons may not localize on a single Cu site, but are rather extended on the ladders and hence S_0 is reduced.

B. Analyses of impurity-induced staggered polarization (IISP)

Fujiwara *et al.* reported the Cu NMR study on the Zn doping ($x=0.0025$ and 0.005).[27] A correlation length ξ_s/a for IISP in $T=30$–40 K was suggested to be much longer than $\xi_0/a\sim3$ predicted theoretically.[18,22–25] However, the observed NMR spectrum was not fit by assuming a form of $S_i=(-1)^i S_0 \exp(-r_i/\xi_s)$ at a distance r_i from the impurity. By contrast, here is presented that the Cu NMR spectra exhibiting the Lorentzian shape are fit by assuming a *regular* distribution of impurities and S_0's on the ladders. Namely, provided that the S_0 (impurity) at $l=0$ and the impurity (S_0) at $l=L$ are located in $0\leqslant l\leqslant L-1$ $(1\leqslant l\leqslant L-1)$ for the A leg (B leg), ${}^A S_l$ (${}^B S_l$) at a distance l is given by

$$ {}^A S_l=(-1)^l S_0 \exp\left(\frac{-la}{\xi_s}\right) + (-1)^{L-l} S_0 \exp\left(\frac{-(L-l)a}{\xi_s}\right) \quad (\text{for } A \text{ leg}), \tag{2}$$

$$ {}^B S_l=(-1)^{l+1} S_0 \exp\left(\frac{-la}{\xi_s}\right) + (-1)^{L-l+1} S_0 \exp\left(\frac{-(L-l)a}{\xi_s}\right) \quad (\text{for } B \text{ leg}). \tag{3}$$

In high T, we model L as an odd number so that the IISP is canceled out around the middle Cu sites between the S_0's on the A and B leg. If a staggered polarization remained finite around the center between S_0's in the case of L being an even number, three peaks might emerge in the NMR spectrum. This is, however, not the case because the observed NMR spectrum is of the Lorentzian type. In this context, regardless of whether a number of lattice between the impurities is odd or even, we expect that a thermal average of IISP would be canceled out around the middle Cu sites at high T.

Sign of local susceptibility χ_l' at a l site changes alternately with varying l as expressed by

$$\chi_l'(T)=\frac{S_l(|S_l|+1)g^2\mu_B^2}{3k_BT}, \tag{4}$$

where μ_B and k_B is the Bohr magneton and Boltzmann's constant, respectively. The g value is 2. The relation between the resonance field H_{res}^l and χ_l' is expressed as

$$H_{res}^l=H_0\left(1+\frac{A_c\chi_l'(T)}{\mu_B}\right), \tag{5}$$

where H_0 is the magnetic field at the peak of ^{65}Cu NMR spectrum [the (3/2↔1/2) transition]. The hyperfine coupling constant parallel to the c axis was previously reported as $A_c=-120$ kOe/μ_B.[5] Each H_{res}^l undertakes a distribution of EFG, $^{65}\Delta H_c$. Eventually, a spectral intensity $I(H)$ is given by

$$I(H)=\sum_{l=0}^{L-1} G({}^A H_{res}^l)+\sum_{l=1}^{L-1} G({}^B H_{res}^l), \tag{6}$$

where $G(H)$ represents the Gaussian distribution. $S_0=1/2$ is fixed for the Zn and Ni doping and $S_0=1/4$ for the La doping. The NMR spectra are fit by solid curves in Figs. 4 (Zn doping) and 5 (La doping). A fitting parameter is only ξ_s/a that is T independent. For the Zn doping, $^{65}\Delta H_c$ and L for $x=0.001$ (0.02) are 0.17 kOe (0.46 kOe) and 499 (25), respectively. As seen in Fig. 4(a) for $x=0.02$, several satellite structures in $I(H)$ become appreciable with decreasing T. In the reality, however, it is likely that some distribution of Zn smears out the satellite structures in $I(H)$ as $\chi_l'(T)$ increases upon cooling. In Fig. 4(a), the $I(H)$ for $\xi_s/a=3$ is indicated by dashed curves. Solid curve represents a best fit with $\xi_s/a=4.5$. For $x=0.001$, it is surprising that the spectrum indicated in Fig. 4(b) is extraordinarily broadened at 4.2 K. The solid curve in the figure traces the $^{65}I(H)$ with $\xi_s/a=50$. In order to fit the spectrum at 4.2 K, it is necessary to incorporate $^{63}I(H)$ in addition to $^{65}I(H)$. Dashed curve traces a sum of $^{65}I(H)$ and $^{63}I(H)$. With this fixed $\xi_s/a=50$, the spectra in $T=4.2$–203 K were well fit as shown in Fig. 4(b). The spectrum for the Ni doping ($x=0.02$) is also fit as well as in the Zn doping ($x=0.02$) by assuming the same $\xi_s/a=4.5$ and $L=25$ but incorporating a smaller $^{65}\Delta H_c=0.36$ kOe.

For the La doping in $x=0.01$–0.03, the spectra are not fit by assuming $S_0=1/2$ but $S_0=1/4$ as shown in Figs. 5(a) ($x=0.03$) and 5(b) ($x=0.01$). Here $^{65}\Delta H_c$ and L for $x=0.03$ (0.01) are 0.30 (0.21) kOe and 33 (99), respectively. An unpaired moment reduced to $S_0=1/4$ for the La doping is because the La impurity replacing the Sr site is expected to dope electrons onto two ladders adjacent to the Sr layer.

In Fig. 6, ξ_s/a's are plotted against mean distances $D_{AV}=1/(2x)$ on the A and B leg for the Zn and Ni doping and $D_{AV}=1/x$ for the La doping. These ξ_s/a's for the Zn and Ni doping give a possible minimum values because $S_0=1/2$ is a possible maximum value. For $S_0<1/2$, ξ_s/a could be larger. Dashed linear line indicates a formula of $\xi_s/a=A+BD_{AV}$ with $A\sim2.5$ and $B\sim0.1$ that is a best fit to the data in $x=0.001$–0.02 for the Zn and Ni doping. Imada and Iino have examined IISP and AF-LRO based on the scaling theory and the quantum Monte Carlo (QMC) calculations involving an effect of interladder coupling.[23] They proposed that the strong-coupling 3D scaling behavior governed by the quantum criticality in Sr123 dominates the magnetic properties of induced moments in the Zn doping.[26] However, the NMR spectra for the impurity-doped Sr123 are well fit by assuming the quasi-1D exponential variation of IISP along the two-leg. This result supports that the quasi-1D magnetic nature is kept for $0.001\leqslant x\leqslant0.02$.

Laukamp *et al.* proposed that introducing spin vacancies prunes or reduces the number of possible resonating spin-singlet configurations and this enlarges the spin correlations.[28] It was indicated that all spins of ladder cluster

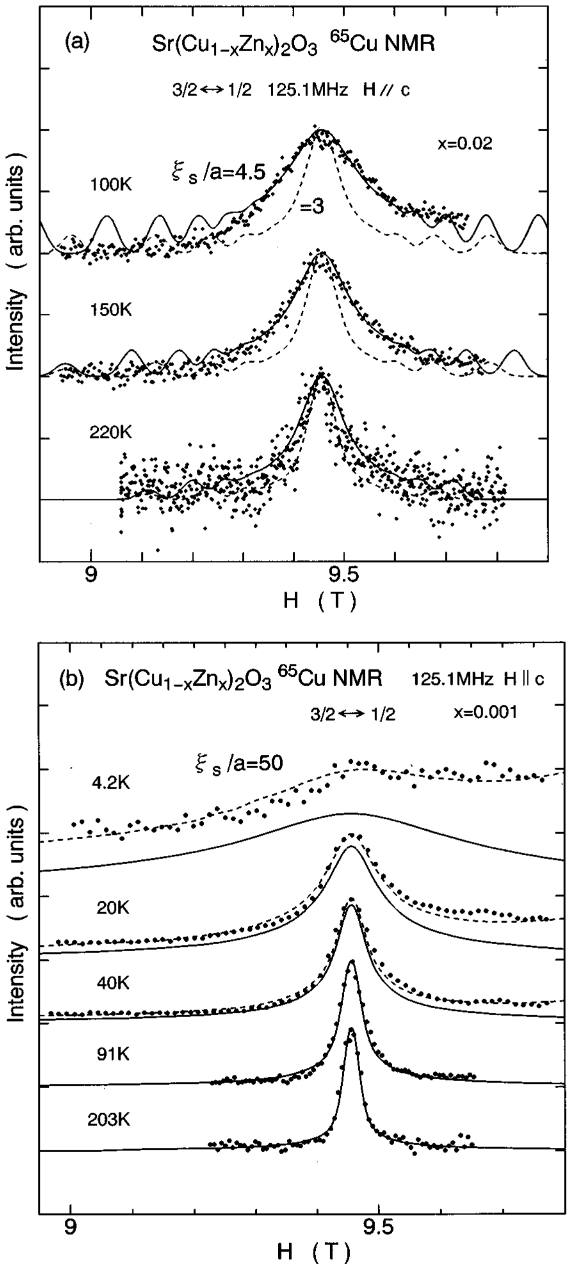

FIG. 4. T dependence of the ^{65}Cu spectrum $[(3/2\leftrightarrow 1/2)$ transition$]$ for the Zn doping with (a) $x=0.02$, and (b) $x=0.01$. For (a), solid (dashed) curve indicates the Lorentzian simulation (LS) with $\xi_s/a=4.5(3)$. For (b), solid curves in $T=4.2$–203 K indicate LS where $\xi_s/a=50$ is fixed. Note that the T dependence of the spectrum originates from that of the susceptibility for unpaired spins grows up following the Curie law. Dashed curves in $T=4.2$–40 K represent LS where its overlapping with the ^{63}Cu spectrum $[(3/2\leftrightarrow 1/2)$ transition$]$ is incorporated. Full details of LS are given in the text.

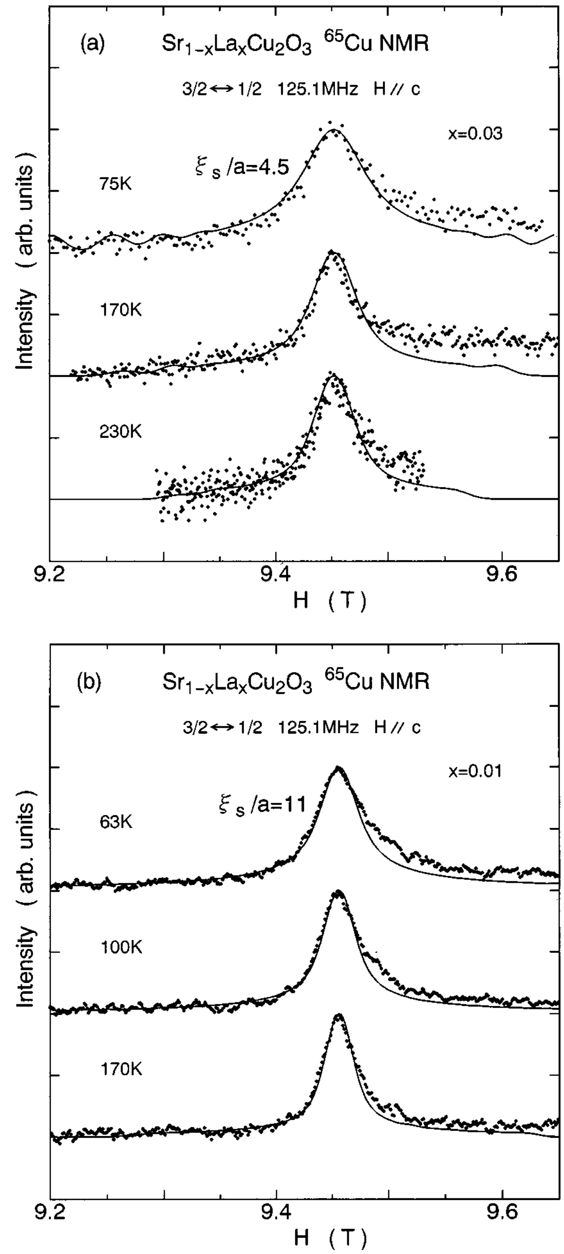

FIG. 5. T dependence of the ^{65}Cu NMR spectrum $[(3/2\leftrightarrow 1/2)$ transition$]$ for the La doping with (a) $x=0.03$, and (b) $x=0.01$. For (a) and (b), solid curves indicate the Lorentzian simulation (LS) with $\xi_s/a=4.5$ and 11, respectively. Full details of LS are given in the text.

with a (2×50) finite size remains finite in the case of $J_\perp/J_0=0.5$ and $\xi_0/a\sim 8$ with $x=0.014$.[28] Here $J_\perp(J_0)$ is the exchange constant along the rung (leg). Furthermore, they suggested that the enlarged AF correlation can stabilize a 3D Néel order once a weak interladder interaction is incorporated.

In this paper, however, we have found that IISP is significantly enlarged with its exponential decay constant increasing as $\xi_s/a=A+BD_{AV}$ where $D_{AV}=1/2x$ (Zn and Ni doping) and $D_{AV}=1/x$ (La doping). Therefore ξ_s/a is larger than $\xi_0/a\sim 8$ in $x=0.001$–0.005. It may be due to this difference between ξ_s and ξ_0 that numerical theoretical treatments failed to explain the emergence of AF-LRO quantitatively.

IV. NQR RESULTS AND DISCUSSION

A. Analyses of Cu NQR spectrum probing AF-LRO

First, we present in Fig. 7 the ^{63,65}Cu NQR spectra at 1.4 K and $H=0$ for the La doping in $x=0.01$–0.03. For the ^{63}Cu (^{65}Cu) isotope, the natural abundance is 69.09 (30.91)

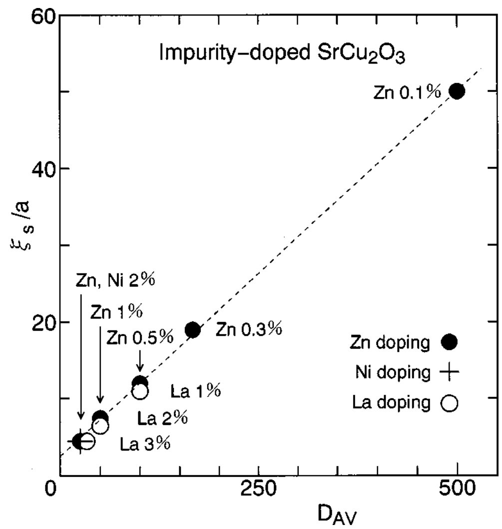

FIG. 6. Plot of correlation length ξ_s/a of IISP against $D_{AV}=1/(2x)$ for the Zn and Ni doping and $D_{AV}=1/x$ for the La doping. Dashed line is a fit with the form of $\xi_s/a=A+BD_{AV}$ for the Zn and Ni doping where $A\sim2.5$ and $B\sim0.1$.

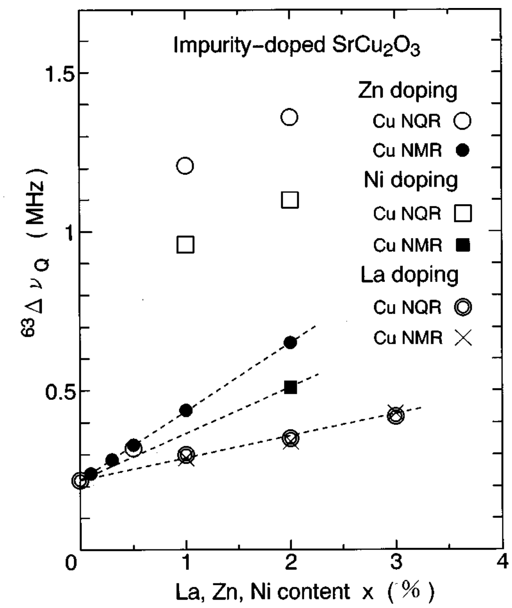

FIG. 8. Impurity concentration x dependence of ${}^{63}\Delta\nu_Q$(NQR) for the La and Zn doping. ${}^{63}\Delta\nu_Q$(NMR) is estimated using Eq. (2) with ${}^{65}\Delta H_c$ at $T\rightarrow\infty$ in ${}^{65}\Delta H$ vs $1/T$ plot in Fig. 2. The half width at half maximum ${}^{63}\Delta\nu_Q$(NQR) of the NQR spectrum in Fig. 9 is also shown for the Zn and Ni doping ($x=0.01$ and 0.02) which exhibit the AF-LRO.

and the ratio of the nuclear quadrupole moment is ${}^{63}Q/{}^{65}Q=0.211/0.195$. Solid curves indicate the Gaussian simulations of two Cu NQR spectra by adjusting two parameters of ^{63}Cu NQR frequency, ${}^{63}\nu_Q$ and full width at half maximum (FWHM), ${}^{63}\Delta\nu_Q$. ${}^{63}\nu_Q$ is almost independent of x, whereas ${}^{63}\Delta\nu_Q$(NQR) increases linearly from 0.22 MHz ($x=0$) to 0.42 MHz ($x=0.03$) as indicated in Fig. 8. ${}^{63}\Delta\nu_Q$(NMR) is also estimated from the ${}^{65}\Delta H_c$ in the NMR experiment through the relation of

$$ {}^{63}\Delta\nu_Q(\mathrm{NMR})=\frac{{}^{63}Q\,{}^{65}\nu_Q^{65}\Delta\nu_c}{{}^{65}Q\,{}^{65}\nu_c}=\frac{{}^{63}Q\,{}^{63}\nu_Q\,{}^{65}\Delta H_c\,{}^{65}\gamma}{2\pi\,{}^{65}Q\,{}^{63}\nu_c}, \tag{7} $$

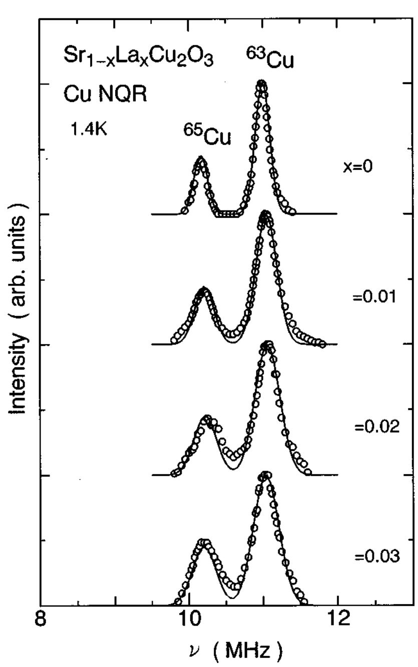

FIG. 7. The Cu NQR spectra for $Sr_{1-x}La_xCu_2O_3$ ($x=0$, 0.01, 0.02, and 0.03) at 1.4 K. Solid curves indicate Gaussian simulations (GS). Full details of GS are given in the text.

where ${}^{63}\nu_Q/{}^{63}\nu_c={}^{65}\nu_Q/{}^{65}\nu_c=11.00/10.15$. As seen in Fig. 8, ${}^{63}\Delta\nu_Q$(NMR) is in good agreement with ${}^{63}\Delta\nu_Q$(NQR). It is apparent that the FWHM for the La doping is dominated by the distribution of EFG originating from the random mixture of Sr and La atoms. The NQR spectra in $x=0.01$–0.03 provide no evidence for an AF-LRO at 1.4 K.

Next, the Cu NQR spectra for the Zn doping for $x=0$, 0.005, 0.01, and 0.02 are shown in Fig. 9. The spectral shape exhibits a drastic change between $x=0.005$ and 0.01. The trapezoidlike spectra for the Zn doping ($x=0.01$ and 0.02) exclude a spin-glass freezing. This is because such characteristic shapes are only reproduced by assuming that a rather uniform H_{int} acts on the Cu nuclei in the ladders. If spins induced only near by impurities were frozen, most Cu nuclei away from S_0 should be not influenced due to a spin-glass freezing and hence two peaks at ${}^{63}\nu_Q$ and ${}^{65}\nu_Q$ could remain traced in the NQR spectrum. This is, however, not the case. Therefore the significantly broadened NQR spectrum signals an onset of AF-LRO at 1.4 K in the Zn and Ni doping. Another evidence for AF-LRO is obtained from the x dependence of T_{2G}^{-1} at 1.4 K. As seen in Fig. 10, T_{2G}^{-1} for the Zn doping changes markedly between $x=0.005$ and 0.01, while that for the La doping has no remarkable change up to $x=0.03$. The increase in T_{2G}^{-1} at $x=0.005$ is likely due to the fact that $T=1.4$ K is already close to a possible AF ordering temperature T_N for $x=0.005$.

The NQR spectrum is fit by combining the Gaussian distributions of EFG and H_{int}, ${}^{63}\Delta\nu_Q$ and ΔH_{int}, and incorporating the split of the NQR spectrum due to H_{int}, $\Delta\nu_{\alpha,\beta}$. This simulation leads to an estimate of H_{int} for the Zn and Ni doping ($x=0.01$ and 0.02). The nuclear-spin Hamiltonian for ^{63,65}Cu ($I=3/2$) at $H=0$ is described in terms of the eqQ and the Zeeman interaction as

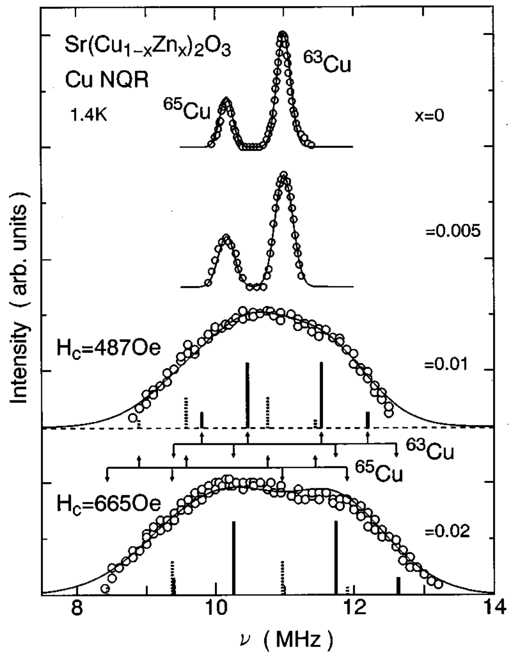

FIG. 9. x dependence of the Cu NQR spectrum for the Zn doping ($x=0$, 0.005, 0.01, and 0.02) at 1.4 K. Solid curves for $x=0$ and 0.005 indicate the Gaussian simulations (GS). For $x=0.01$ and 0.02, solid (dotted) bar indicates the intensity of two sets of the NQR transitions of ^{63}Cu (^{65}Cu) split due to the internal field H_c associated with the AF-LRO. Solid curve indicates GS for two sets of NQR transitions with $H_c=487$ (665) Oe and $^{63}\Delta\nu_Q$(NQR) $=1.21\,(1.36)$ MHz for $x=0.01$ (0.02). Note that $^{63}\Delta\nu_Q$(NQR) is larger than $\Delta\nu_Q(\mathrm{NMR})=0.44\,(0.65)$ MHz for $x=0.01$ (0.02) as shown in Fig. 8, including some distribution of the internal field ΔH_c.

$$H_Q=\frac{e^2qQ}{4I(2I-1)}\left[3I_z^2-I(I+1)+\frac{\eta(I_+^2+I_-^2)}{2}\right],\qquad(8)$$

$$H_Z=-\gamma\hbar\mathbf{I}\cdot\mathbf{H}_{\mathrm{int}},\qquad(9)$$

where γ is the ^{63,65}Cu gyromagnetic ratio. In Eq. (8), the asymmetry parameter η for the EFG tensor is defined by

$$\eta\equiv\frac{V_{XX}-V_{YY}}{V_{ZZ}},\qquad(10)$$

where $|V_{ZZ}|(\equiv eq)\geqslant|V_{YY}|\geqslant|V_{XX}|$. The z axis is the principal axis along which EFG gives a maximum value and $V_{ZZ}\sim\nu_c\gg\gamma H_{\mathrm{int}}$. By resolving H_Q exactly and treating H_Z in terms of the first-order perturbation, we calculated the eigenenergies of four nuclear-spin levels. A single NQR spectrum is separated into two sets of spectra. Half value of their frequency separation $\Delta\nu_{\alpha,\beta}/2$ is given by

$$\begin{array}{lll} & H_{\mathrm{int}} \quad \Delta\nu_\alpha/2 & \Delta\nu_\beta/2,\\ a\ \text{axis} & (1-\eta)\rho\gamma H_a/2\pi & \gamma H_a/2\pi,\\ b\ \text{axis} & \gamma H_b/2\pi & (1+\eta)\rho\gamma H_b/2\pi,\\ c\ \text{axis} & \gamma H_c/2\pi & 2\rho\gamma H_c/2\pi,\end{array}\qquad(11)$$

where

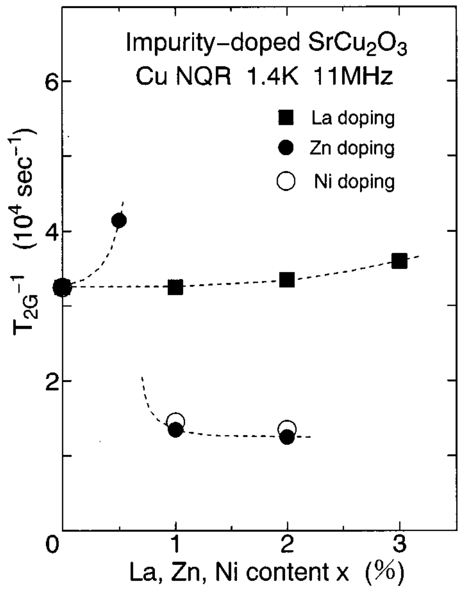

FIG. 10. x dependence of the Gaussian spin-echo decay rate T_{2G}^{-1} at 1.4 K for the Zn, Ni, and La doping. Dashed curves are guides for the eye.

$$\rho=\left(1+\frac{1}{3}\eta^2\right)^{1/2}=\frac{\nu_Q}{\nu_c}.\qquad(12)$$

Here a, b, and c denote the crystal axes for Sr123. $\nu_a=-1.46$ MHz, $\nu_b=-8.69$ MHz, and $\nu_c=10.15$ MHz were reported previously.[5] From Eqs. (10) and (12) together with $\nu_{a,b,c}$, $\eta\sim0.72$ is estimated. Concerning a possible direction of H_{int}, we assume all the cases, H_a, H_b, and H_c. The transition probability P was calculated under the condition that a distribution of the radio-frequency field $H_1(\theta)$ in the powder is averaged over the polar angle θ between H_1 and each axis. An intensity of P is indicated in Fig. 9 by a height of bold solid (^{63}Cu) and dotted (^{65}Cu) bars for H_c. Solid curve represents a simulation decomposed of four Gaussian curves whose width is a sum of $^{63}\Delta\nu_Q$ and ΔH_{int}, $^{63}\Delta\nu_Q$(NQR) for $x=0.01$ and 0.02. As shown in Fig. 8, $^{63}\Delta\nu_Q$(NQR) for the Zn doping ($x=0.01$ and 0.02) are considerably larger than the $^{63}\Delta\nu_Q$(NMR)'s that was estimated using the $^{65}\Delta H_c$'s (see Fig. 2). Since $^{63}\Delta\nu_Q$(NQR) $>{}^{63}\Delta\nu_Q$(NMR), the $^{63}\Delta\nu_Q$(NQR)'s for $x=0.01$ and 0.02 cannot be attributed only to the distribution of EFG, but is rather dominated by some inhomogeneous distribution of internal field H_{int}, ΔH_{int}. H_{int} is produced by an AF-LRO. The results for the Ni doping were shown to be almost the same as for the Zn doping.

Fitting parameters for the Zn doping are summarized in Table I. From Eq. (11) using $A_{a,b}=48$ kOe/μ_B and $A_c=-120$ kOe/μ_B,[5] a size of AF moment is estimated from the relation of $\langle\mu\rangle_{a,b,c}=H_{a,b,c}/A_{a,b,c}$. $\langle\mu\rangle_a$, $\langle\mu\rangle_b$, and $\langle\mu\rangle_c$ are plotted in Fig. 11 together with T_N.[16] The magnitude of $\langle\mu\rangle$ is almost the same for the Zn and Ni doping. Recently, Azuma *et al.* have reported from the susceptibility $\chi(T)$ measurement on the c-axis oriented powders that the direction of AF moments is in the Cu_2O_3 planes.[30] In this case, $\langle\mu\rangle_a$ and $\langle\mu\rangle_b$ is in a range of 0.01–0.04μ_B, and increases as x increases.

TABLE I. Fitting parameters of the Cu NQR spectra for the Zn doping ($x=0.01$ and 0.02) in Fig. 9. Here, $\Delta\nu_\alpha$, $^{63}\Delta\nu_Q$(NQR), $H_{a,b,c}$, and $\langle\mu\rangle_{a,b,c}$ denote the separation due to $H_{\rm int}$, the full width at half maximum of ^{63}Cu NQR spectrum, $H_{a,b,c}$, and average AF moments around the center between impurities, respectively.

	Axis	$\Delta\nu_\alpha/2$ (MHz)	$^{63}\Delta\nu_Q/2$ (MHz)	H (Oe)	$\langle\mu\rangle(10^{-2}\mu_B)$
	a	0.60	1.21	$H_a=1755$	3.66
Zn 1%	*b*	0.54	1.22	$H_b=479$	1.00
	c	0.55	1.21	$H_c=487$	0.41
	a	0.80	1.34	$H_a=2340$	4.88
Zn 2%	*b*	0.74	1.37	$H_b=656$	1.37
	c	0.75	1.36	$H_c=665$	0.55

B. Spatial variation of AF moments and Néel temperature (T_N)

The NQR results point to the presence of rather *uniform* AF moment, which is not consistent with the result that the IISP decreases *exponentially*. Note that the Cu NQR signal in the vicinity of the impurities is out of detection because $H_{\rm int}$'s at the Cu sites around the impurity are distributed with larger values than around the middle Cu sites between them. Figure 12 indicates the *x* dependence of the integrated intensity $II(\nu)$ of NQR spectrum at 1.4 K in Fig. 9. This shows that only 24% and 17% of the total Cu sites contribute to the observed NQR spectrum for the Zn doping ($x=0.01$ and 0.02, respectively).

In Figs. 13(a) and 13(b), solid curve represents a spatial variation of $|\mu_l|=g|S_l|$ $(g=2)$ at 1.4 K corresponding to Eq. (2) with $L=25$, $\xi_s/a=4.5$ and $L=50$, $\xi_s/a=8$, respectively. The region marked by the slash lines in Fig. 13 corresponds to only 17% ($x=0.02$) and 24% ($x=0.01$) of the total Cu sites. By assigning $\langle\mu\rangle_a=0.0366(0.0488)\mu_B$ for $x=0.01$ (0.02) at 1.4 K at the center between the impurities, $\mu_{AF}\sim0.41(0.39)\mu_B$ $[S_{AF}\sim0.21(0.20)]$ are deduced. These values are consistent with the results calculated by Mikeska *et al.*[25] and Laukamp *et al.*[28] We thus find that the IISP is spontaneously ordered below T_N. As expected, the exponential decrease of AF moments along the leg is equivalent to that of IISP. This 1D nature of IISP allows us to be based on a weakly coupled quasi-1D (WC-Q1D) model in evaluating T_N.

For WC-Q1D ladders, T_N might be dominated by an effective exchange coupling between two S_0's along the leg, given by

$$T_N(\text{WC-Q1D})=J_0e^{-D_{AV}/(\xi_s/a)}. \tag{13}$$

Here J_0 is the nearest-neighbor exchange coupling along the leg. Assuming $J_0=2000$ K estimated from the $\chi(T)$ in Sr_2CuO_3 and $SrCuO_2$ (Ref. 29) and using ξ_s/a's obtained from the NMR measurements as shown in Fig. 6, T_N(WC-Q1D) is plotted against *x* for the Zn doping by cross marks in Fig. 14. For $x=0.01$ (0.02), T_N(WC$-$Q1D) $=2.6(7.7)$ K is in quantitative agreement with T_N(exp) $=3.0(5.8)$ K.[16] If $\xi_s/a=4.3$ is assigned within experimental

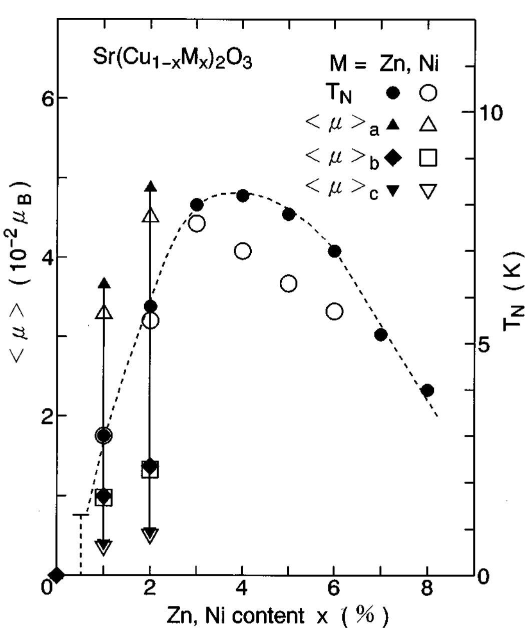

FIG. 11. Average AF moments $\langle\mu\rangle_{a,b,c}$ around the center between the impurities for the Zn and Ni doping ($x=0.01$ and 0.02) together with the *x* dependence of T_N in $x=0$–0.08. *a*, *b*, and *c* denote the crystal direction. Solid lines indicate a range of $\langle\mu\rangle_a$, $\langle\mu\rangle_b$, and $\langle\mu\rangle_c$. Dashed line is a guide for the eye to the *x* dependence of T_N for the Zn doping.

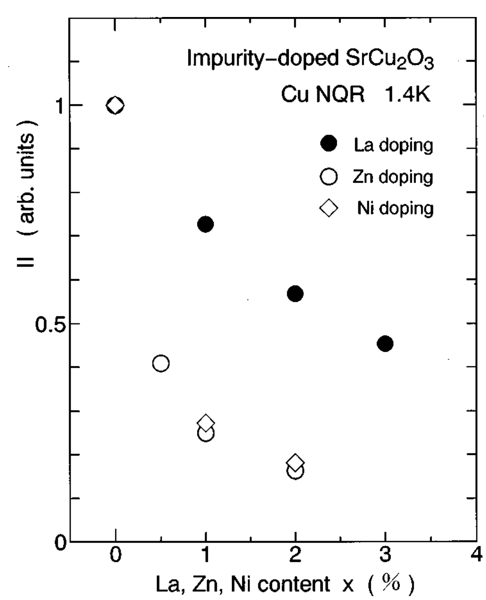

FIG. 12. *x* dependence of the integrated intensity $II(\nu)$ of the NQR spectra in Figs. 7 and 9 for the Zn, Ni, and La doping at 1.4 K.

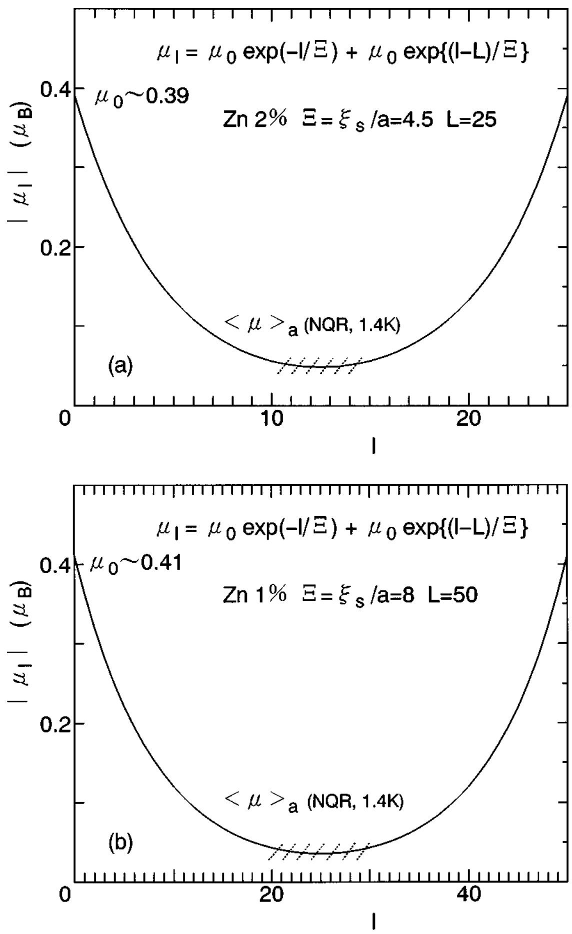

FIG. 13. Exponential decrease of AF moments $|\mu_l|$ in Eqs. (2) and (3) for the Zn doping with (a) $x=0.02$ and (b) $x=0.01$ at 1.4 K. Slash line indicates the central region between impurities where the Cu NQR spectrum was observable. (a) $x=0.02$, $\langle\mu\rangle_a=0.0488$, $\mu_{AF}=0.39\mu_B$ ($S_{AF}\sim0.20$), $\xi_s/a=4.5$, and $L=25$. (b) $x=0.01$, $\langle\mu\rangle_a=0.0366\mu_B$, $\mu_{AF}=0.41\mu_B$ ($S_{AF}\sim0.21$), $\xi_s/a=8$, and $L=50$.

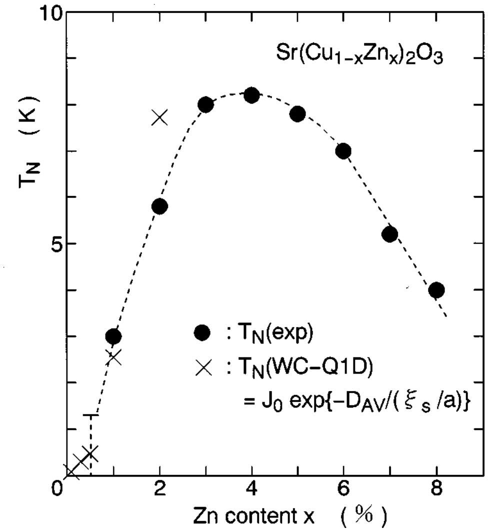

FIG. 14. x dependence of the Néel temperature T_N predicted from the formula $T_N=J_0\exp(-D_{AV}/(\xi_s/a))$ (Ref. 26) based on the weakly coupled quasi-1D model for the Zn doping with $x=0.001$–0.02. $J_0=2000$ K is the nearest-neighbor exchange coupling along the leg. ξ_s/a's were those estimated from the present NMR measurements (see Fig. 6). This model explains the experimental T_N(exp) (solid circles) quantitatively (Ref. 16).

accuracy at $x=0.02$, $T_N(\mathrm{WC-Q1D})=T_N(\mathrm{exp})$ is deduced. We may also predict $T_N(\mathrm{WC-Q1D})=0.09$, 0.31, and 0.48 K for $x=0.001$, 0.003, and 0.005, respectively. On the other hand, there is no evidence for an onset of AF-LRO down to 1.4 K for the La doping, nevertheless ξ_s/a's in $x=0.01$–0.03 are almost equivalent to those in the Zn and Ni doping ($x=0.01$–0.02). This lack of AF-LRO in the La doping may be relevant to the fact that the unpaired spin $S_0\sim1/4$ at the Cu sites around the La impurity is reduced to a half of $S_0\sim1/2$ in the Zn and Ni doping.

From the x dependence of $T_N=a\exp(-b/x)$ in Zn-doped $CuGeO_3$, it was concluded that there is no critical concentration for the occurrence of AF-LRO.[31] This indicates that the dimerization sustains the coherence of IISP in this system, which was consistent with the theory of the impurity-doped spin-Peierls system.[15] The T_N and the IISP in this system are considered to be determined by a relative large and *uniform* interchain interaction with a unique ''soliton length'' $\xi_0/a=7.78$ relevant to $CuGeO_3$ with $J_0\sim100$ K and a spin gap, $\Delta\sim25$ K.

The Q1D nature of IISP in the impurity-doped Sr123 is because the staggeredness is perfectly maintained by the quantum coherence in the gapped spin-1/2 Heisenberg two-leg ladder system. The impurity that depletes a single spin breaks the singlet formation locally and eventually the induced moments partially lift the spin frustration at the interface around S_0. It may be due to this weak interladder interaction to enhance the Q1D-IISP of which the correlation length $\xi_s/a=A+BD_{AV}$ increases with decreasing x. We remark that T_N is determined by a strength of interladder interaction and a size of S_0.

V. CONCLUSION

On the base of the extensive Cu NMR and NQR studies on the impurity-doped spin-1/2 two-leg spin-ladder $SrCu_2O_3$ with the gap, we have clarified the characteristics of Q1D impurity-induced staggered polarizaton (IISP) and the onset of AF-LRO in the Zn and Ni doping ($x=0.01$ and 0.02), not for the La doping up to $x=0.03$. We have found that the correlation length ξ_s/a of IISP that is T independent is scaled to a mean distance D_{AV} between the impurities. An experimental relation of $\xi_s/a=A+BD_{AV}$ with $A\sim2.5$ and $B\sim0.1$ has been obtained in $x=0.001$–0.02 for the Zn and Ni doping. $\xi_s/a\sim50$ for $D_{AV}=500$ in the Zn doping ($x=0.001$) is two orders of magnitude longer than $\xi_0/a\sim3$–8 in Sr123.[1,2,32] Based on the computational techniques on the 2×50 cluster of the ladders,[28] it was shown that all spins of the (2×50) cluster have nonvanishing AF susceptibility in the case of $J_\perp/J_0=0.5$ (Ref. 32) and $x=0.014$. We suggest that the striking experimental relation $\xi_s/a=A+BD_{AV}$ is relevant to some nonuniform weak interladder interaction because the magnetic frustration at the interface is partially lifted around impurities.

From the comprehensive analyses on the broadened Cu NQR spectra for the Zn and Ni doping, it was shown that the AF moments $\langle\mu\rangle_a=0.0366(0.0488)\mu_B$ for $x=0.01$ (0.02) are rather uniform around the middle Cu sites between the impurities. By assuming an unpaired spin $S_{AF}\sim0.21$ (0.20) next to the impurity at 1.4 K, the exponential decrease of AF moments has been found to be almost equivalent to those in the IISP with $\xi_s/a=8$ $(x=0.01)$ and 4.5 $(x=0.02)$ for the Zn and Ni doping. This quasi-1D nature of IISP has provided experimental support that the interladder interaction is in the weakly coupled quasi-1D (WC-Q1D) regime, but not in the strongly coupled 3D regime proposed on the scaling theory.[26] The formula of $T_N=J_0\exp(-D_{AV}/(\xi_s/a))$ derived based on the WC-Q1D model explains quantitatively the experimental T_N values in the Zn and Ni doping and predicts $T_N\sim0.09$ K for $x=0.001$ using $J_0=2000$ K. On the other hand, there is no evidence of AF-LRO for the La doping ($x=0.01$–0.03) down to 1.4 K, although their ξ_s/a's are almost equivalent to those in the Zn and Ni doping ($x=0.01$–0.02). We propose that the Q1D-IISP is dramatically enhanced by the interladder interaction even though so weak, once the impurity breaks up the quantum coherence in the short-range RVB state with the gap. We propose that T_N is determined by a strength of the interladder interaction and a size of S_0.

ACKNOWLEDGMENTS

The authors would like to thank H. Fukuyama, M. Imada, and E. Dagotto for valuable comments and stimulating discussions regarding their theoretical works. S.O. would like also to thank K. Magishi, M. Sakai, and G.-q. Zheng (Osaka University) for experimental assists and Z. Hiroi and M. Iida (Kyoto University) for valuable comments. This work was partly supported by a Grant-in-Aid for Scientific Research (No. 09440138) of the Ministry of Education, Science and Culture of Japan and CREST (Core Research for Evolutional Science and Technology) of Japan Science and Technology Corporation (JST).

[1] T. M. Rice, S. Gopalan, and M. Sigrist, Europhys. Lett. **23**, 445 (1993); S. Gopalan, T. M. Rice, and M. Sigrist, Phys. Rev. B **49**, 8901 (1994); M. Sigrist, T. M. Rice, and F. C. Zhang, *ibid.* **49**, 12 058 (1994).

[2] M. Troyer, H. Tsunetsugu, and D. Würtz, Phys. Rev. B **50**, 13 515 (1994).

[3] Z. Hiroi, M. Azuma, M. Takano, and Y. Bando, J. Solid State Chem. **95**, 230 (1991).

[4] M. Azuma, Z. Hiroi, M. Takano, K. Ishida, and Y. Kitaoka, Phys. Rev. Lett. **73**, 3463 (1994).

[5] K. Ishida, Y. Kitaoka, K. Asayama, M. Azuma, Z. Hiroi, and M. Takano, J. Phys. Soc. Jpn. **63**, 3222 (1994); K. Ishida, Y. Kitaoka, Y. Tokunaga, S. Matsumoto, K. Asayama, M. Azuma, Z. Hiroi, and M. Takano, Phys. Rev. B **53**, 2827 (1996).

[6] M. Azuma, M. Takano, and R. S. Eccleston, J. Phys. Soc. Jpn. **67**, 740 (1998).

[7] E. Dagotto, J. Riera, and D. J. Scalapino, Phys. Rev. B **45**, 5744 (1992); T. Barnes, E. Dagotto, J. Riera, and E. Swanson, *ibid.* **47**, 3196 (1993); A. W. Sandvik, E. Dagotto, and D. J. Scalapino, *ibid.* **53**, R2934 (1996); for review, see E. Dagotto and T. M. Rice, Science **271**, 618 (1996).

[8] R. M. Noack, S. R. White, and D. J. Scalapino, Phys. Rev. Lett. **73**, 882 (1994); S. R. White, R. M. Noack, and D. J. Scalapino, *ibid.* **73**, 886 (1994); C. A. Hayward, D. Poliblac, R. M. Noack, D. L. Scalapino, and W. Hanke, *ibid.* **75**, 926 (1995).

[9] M. Uehara, T. Nagata, J. Akimitsu, H. Takahashi, N. Mōri, and K. Kinoshita, J. Phys. Soc. Jpn. (to be published).

[10] M. Azuma *et al.* (unpublished).

[11] M. Hase, I. Terasaki, and K. Uchinokura, Phys. Rev. Lett. **70**, 3651 (1993); **71**, 4059 (1993).

[12] J. P. Renard *et al.*, Europhys. Lett. **30**, 475 (1995).

[13] L. P. Regnault *et al.*, Europhys. Lett. **32**, 579 (1995).

[14] Y. Sasago *et al.*, Phys. Rev. B **54**, R6835 (1996).

[15] H. Fukuyama, M. Saito, and T. Tanimoto, J. Phys. Soc. Jpn. **65**, 1182 (1996).

[16] M. Azuma, Y. Fujishiro, M. Takano, M. Nohara, and H. Takagi, Phys. Rev. B **55**, R8658 (1997); M. Takano *et al.*, Physica C **282-287**, 149 (1997).

[17] M. Nohara, H. Takagi, M. Azuma, Y. Fujishiro, and M. Takano, J. Phys. Soc. Jpn. (unpublished).

[18] H. Fukuyama, N. Nagaosa, M. Saito, and T. Tanimoto, J. Phys. Soc. Jpn. **65**, 2377 (1996).

[19] H. Fukuyama, in *Proceedings of μSR'96*, Nikko, 1996 [Hyperfine Interact. **104**, 17 (1997)].

[20] M. Saito and H. Fukuyama, J. Phys. Soc. Jpn. **66**, 3258 (1997).

[21] M. C. Martin *et al.*, Phys. Rev. B **56**, 3173 (1997).

[22] Y. Motome, N. Katoh, N. Furukawa, and M. Imada, J. Phys. Soc. Jpn. **65**, 1949 (1996).

[23] Y. Iino and M. Imada, J. Phys. Soc. Jpn. **65**, 3728 (1996).

[24] G. B. Martins, M. Laukamp, J. Riera, and E. Dagotto, Phys. Rev. Lett. **78**, 3563 (1997).

[25] H.-J. Mikeska, U. Neugebauer, and U. Schollwöck, Phys. Rev. B **55**, 2955 (1997).

[26] M. Imada and Y. Iino, J. Phys. Soc. Jpn. **66**, 568 (1997).

[27] N. Fujiwara, H. Yasuoka, Y. Fujishiro, M. Azuma, and M. Takano, Phys. Rev. Lett. **80**, 604 (1998).

[28] M. Laukamp, G. B. Martines, C. Gazza, A. L. Malvezzi, E. Dagotto, P. M. Hansen, A. C. Lopez, and J. Riera, Phys. Rev. B **57**, 10 755 (1998).

[29] N. Motoyama, H. Eisaki, and S. Uchida, Phys. Rev. Lett. **76**, 3212 (1996).

[30] M. Azuma *et al.* (unpublished).

[31] K. Manabe *et al.*, Phys. Rev. B **58**, R575 (1998).

[32] D. C. Johnston, Phys. Rev. B **54**, 13 009 (1996).